PHYSICAL REVIEW B VOLUME 49, NUMBER 23 15 JUNE 1994-I

Tunneling and nonresonant negative differential resistance in narrow-well interband-tunneling devices

Y. Naveh and B. Laikhtman
Racah Institute of Physics, The Hebrew University of Jerusalem, Jerusalem 91904, Israel
(Received 22 February 1994)

We predict the observation of negative differential resistance (NDR) in interband tunneling devices (ITD's) of well width smaller then 100 Å. This strong NDR results from the nature of tunneling in ITD's, and is not related to resonant tunneling. It is inherent to the ITD structure, and should be experimentally observed in any symmetric ITD (including polytype structures). The mechanism is given in terms of simple physical arguments. Rigorous calculations of the current-voltage characteristics of narrow-well ITD's are then made in the framework of the effective-mass approximation.

Vertical transport through multiple type-II semiconductor heterojunctions has been extensively studied in recent years.[1–11] Those structures, now known as interband tunneling devices (ITD's), feature a strong nonlinear behavior of their current-voltage characteristics. At a particular voltage a sharp drop in the current is observed, and the peak-to-valley ratio of this negative differential resistance (NDR), together with the large peak current density, has been suggestive of future device applications of the structures.

When the well-acting material of the ITD is wide enough, the first quantum level in the well is aligned with an allowed energy band in the outer electrodes. In the canonical structure GaSb-InAs-GaSb, this means that the first InAs conduction level E_1 is lower in energy than the GaSb valence-band edge, which is taken as the zero of energy [Fig. 1(a)]. This happens for InAs layer width L larger then about 100 Å. In this case, resonant tunneling through E_1 takes place. It is now established[6] that the mechanism for NDR in wide wells is the voltage-induced raise of the E_1 level above the valence-band edge at the emitter.

Transport through ITD's is generally viewed as a tunneling phenomena. However, contrary to conventional tunneling, carrier energies in the tunneling region are positive with respect to the local potential. In this paper we justify the view of tunneling in ITD's. We then show that at intermediate and high voltages ($V \geq 0.1$ V) an ITD behaves totally different from a conventional tunneling device. In particular we show that strong NDR, which is not related to resonant tunneling, is expected in narrow-well devices. The mechanism for this NDR has been suggested by Taira *et al.*,[3] but was discarded on experimental grounds.[6] However, the experiments were done with low doping levels in the electrodes. We rigorously show here that in the case of heavily doped electrodes, this mechanism for NDR leads to peak currents comparable to those of resonant-tunneling devices. It is the only way to achieve NDR in narrow-well devices, and thus to utilize their advantages, such as small lattice-mismatch effects, and short tunneling time. A nonresonant process should also be faster than a resonant one. We expect this NDR phenomenon to be observed experimentally, and possibly to have an impact on future applications of ITD's.

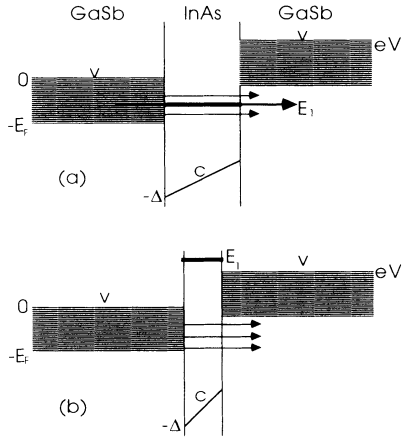

FIG. 1. Tunneling in ITD. (a) $L > 100$ Å: resonant tunneling. (b) $L < 100$ Å: direct interband tunneling. v, c denote valence- and conduction-band edges.

We use a realistic, three-dimensional, effective-mass approximation to calculate the current through the voltage-biased structure. The energy profile of the studied structure, under applied voltage, is shown in Fig. 1(b). From the energy profile alone, one would expect valence states from the outer GaSb electrodes to penetrate the heterojunctions into the InAs conduction band. Indeed, if conventional boundary conditions are used (i.e., the continuity of ψ, $m^{-1}\psi'$, m being the spatial-dependent effective mass), the calculations show that the amplitude of the penetrated envelope functions inside the well are of the order of magnitude of the amplitude of the original valence-band envelope functions. This implies charge transfer towards the well (even for $E_1 > eV$), and results in significant band bending. However, Ando and Mori,[12] and recently Harrison and Kozlov,[13] started from a tight binding model to determine the appropriate boundary conditions that should be used in the effective-mass approximation. The conditions,[13] when applied to extreme type-II heterojunctions, read

$$\begin{aligned} \alpha^{\frac{1}{2}}\psi_v &= \tfrac{1}{2}\left(\gamma - \tfrac{1}{\gamma}\right)\psi_c - \tfrac{a}{4}\left(\gamma + \tfrac{1}{\gamma}\right)\psi_c', \\ \tfrac{a}{2}\alpha^{\frac{1}{2}}\psi_v' &= -\tfrac{1}{2}\left(\gamma + \tfrac{1}{\gamma}\right)\psi_c + \tfrac{a}{4}\left(\gamma - \tfrac{1}{\gamma}\right)\psi_c'. \end{aligned} \quad (1)$$

Here ψ_v, ψ_c are the valence-band and conduction-band envelope functions, evaluated at the boundary. a is the lattice constant, and α is the effective mass ratio,

$$\alpha = \frac{m_c}{|m_v|},$$

m_v being the mass of the heavy holes, which are dominant due to their large density of states. In the specific structure $\alpha = 1/15$. γ is an unknown physical parameter which describes the penetrability of the interface.[13] It is generally assumed that $\gamma = 1$. In that case, the conditions of Ando and Mori[12] are recovered, and ψ on one side is matched to ψ' on the other side.

For any value of γ, Eqs. (1) imply that the amplitude of the envelope function in the InAs well is smaller by a factor of $ka/2$ as compared to the amplitude of the valence-band functions. Only at energies very close to one of the confinement energies E_n is the amplitude in the well larger then the one outside. Within the framework of the effective-mass approximation, $ka \ll 1$. The net result of the interband boundary conditions [Eqs. (1)] is therefore to keep carrier states confined to their original material, with only small (of order $ka/2$) penetration through interfaces. We emphasize that this is true even for $\gamma = 1$, which usually implies complete penetrability of the interface.

These arguments are the reason why one can treat the current through the structure as a tunneling current, and in the case of a wide well, as resonant tunneling through a truly confined level. For a narrow well, the smallness of the relative amplitude inside the well allows us to use flat-band conditions at zero bias.

There is, however, one very important difference between the presently studied structure, and conventional tunneling through a barrier. In the case of a true barrier [Fig. 2(a)], the wave functions in the barrier region are of evanescent type, and tend to increase in magnitude when the effective width and height of the barrier are shrunk by the applied voltage. This behavior renders the transmission coefficient through the barrier to be a monotonous increasing function of the voltage. In our case of ITD [Fig. 2(b)], the states in the well are extended like at $V = 0$. For large applied voltage, i.e., eV larger then the band offset Δ, the well becomes a true barrier for the conduction-band states, and those states become evanescent. Raising the voltage now raises the effective height and width of the barrier, so that the transmission coefficient T decreases with increasing voltage. For small voltages ($eV < E_F, \Delta$), $T(V)$ is a weak function of V. In this case the current should rise linearly with voltage, as in normal tunneling, due to the opening of the allowed-tunneling window $E_F' - E_F$ (see Fig. 3). E_F, E_F' are the quasi-Fermi-levels in the emitter and collector, respectively.

To calculate the current density J through the structure, we used the well-known expression[14]

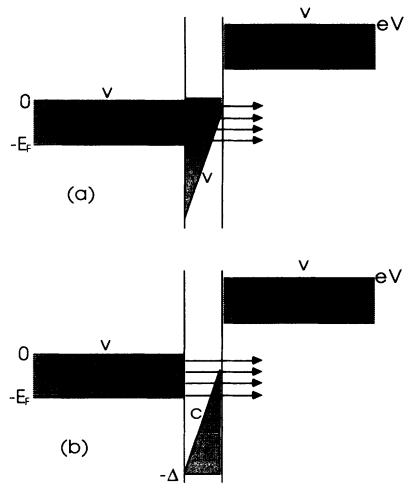

FIG. 2. Tunneling of holes in double heterojunction devices. (a) True tunneling (as in the GaAs-GaAlAs-GaAs system). (b) Interband tunneling. Shaded regions represent the true barriers, under which the quantum states are evanescent.

$$J = \frac{e}{4\pi^3\hbar}\int_0^\infty dk_A \times \int_0^\infty d^2k_\perp\,[f(E) - f(E')]\,T(E,E')\frac{\partial E}{\partial k_A}, \quad (2)$$

where k_A, $k_\perp$ are the vertical and in-plane wave numbers, respectively, $f(E)$ is the hole Fermi function, and

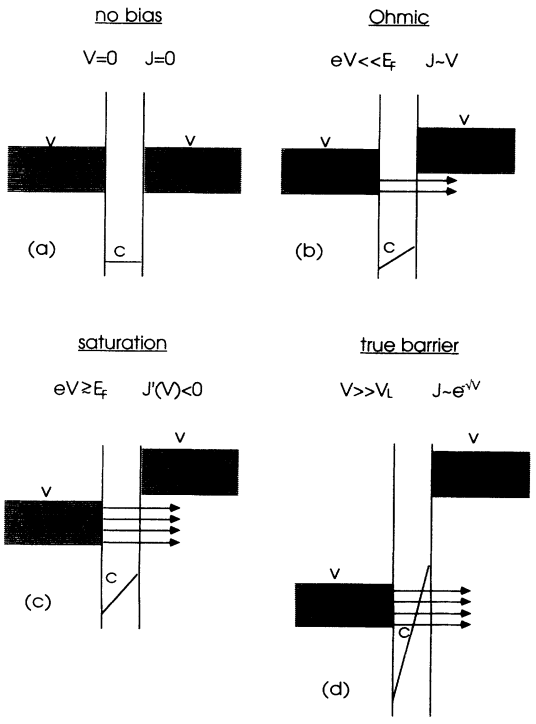

FIG. 3. The evolution of the energy profile of ITD with increasing voltage. Each snapshot represents a different regime in the J-V characteristics, as described in the text.

$$E = -\frac{\hbar^2 k_A^2}{2|m_v|} - \frac{\hbar^2 k_\perp^2}{2|m_v|},$$

$$E' = E - eV,$$

are the initial and final hole energies, each with respect to the local valence-band edge. Because of the reasons mentioned above, band bending and charge redistribution are neglected. Thus, the potential inside the well is assumed to be linear.

The difference in effective masses between the outer electrodes and the well implies a strong interaction between k_A and $k_\perp$ for a given energy state in the well. Therefore, $T(E, E') = T(k_A, k_\perp, V)$ is strongly nonseparable in k_A, $k_\perp$.

The transmission coefficient through the structure was calculated with the help of the boundary conditions [Eq. (1)], and for a narrow well ($L < 100$ Å) it is expressed in terms of Airy functions Ai, Bi as

$$T(k_A, k_\perp, V) = \frac{k_A^2 \bar{k}_B^2 a^4 (1-\delta^2)^2}{4\pi^2 [\mathrm{Ai}(\eta^-)\mathrm{Bi}(\eta^+) - \mathrm{Ai}(\eta^+)\mathrm{Bi}(\eta^-)]^2}, \tag{3}$$

where the following definitions are used

$$\delta = \frac{\gamma^2 - 1}{\gamma^2 + 1},$$

$$\bar{k}_B L = \left(\frac{V}{V_L}\right)^{\frac{1}{3}},$$

$$eV_L = \frac{\hbar^2}{2m_c L^2},$$

$$\eta^\pm = \bar{k}_B \left(\pm\frac{L}{2} - x_t\right)$$

in which x_t is the classical turning point,

$$x_t = \left(\frac{\Delta + E - \frac{\hbar^2 k_\perp^2}{2m_c}}{eV} - \frac{1}{2}\right) L. \tag{4}$$

Equation (3) assumes nonresonance conditions. When resonance occurs (in wide wells), the denominator in Eq. (3) vanishes, and terms of higher order in $k_A a$ and $\bar{k}_B a$, which are neglected here, limit the transmission.

In the case of small carrier density, i.e.,

$$E_F \ll \frac{\alpha}{\alpha + 1}\Delta \tag{5}$$

the arguments of the Airy functions are approximated by

$$\eta^- \approx -\bar{k}_B L \frac{\Delta}{eV}, \qquad \eta^+ \approx \bar{k}_B L \left(1 - \frac{\Delta}{eV}\right),$$

and an analytical result for the current density in zero temperature is obtained,

$$J = \frac{e\hbar a^4 (1-\delta^2)^2 k_F^6}{192\pi^4 m_v} \frac{\bar{k}_B^2}{[\mathrm{Ai}(\eta^-)\mathrm{Bi}(\eta^+) - \mathrm{Ai}(\eta^+)\mathrm{Bi}(\eta^-)]^2} \times \left[1 - \left(1 - \frac{eV}{E_F}\right)^3 \Theta(E_F - eV)\right]. \tag{6}$$

Here k_F is the Fermi wave number and $\Theta(x)$ is 1 for $x \geq 0$ and 0 otherwise.

The behavior of the J-V characteristics can now be analyzed in different voltage regimes. First, for $eV \ll \Delta$, the turning point is far from the well, $x_t \gg L$. The asymptotic behavior of the Airy functions now gives

$$\frac{\bar{k}_B^2}{[\mathrm{Ai}(\eta^-)\mathrm{Bi}(\eta^+) - \mathrm{Ai}(\eta^+)\mathrm{Bi}(\eta^-)]^2} = \frac{\pi^2 k_B^2}{\sin^2(k_B L)},$$

where k_B is defined by

$$E = \frac{\hbar^2 k_B^2}{2m_c} + \frac{\hbar^2 k_\perp^2}{2m_c} - \Delta + \frac{eV}{2}.$$

Substituting this in Eq. (6) reproduces the result obtained for a flat potential raise of $eV/2$ throughout the well. The results at all regimes are thus summarized:

$$\begin{aligned}
&\text{(I)} \quad eV \ll E_F, \quad J \propto V; \\
&\text{(II)} \quad eV \gtrsim E_F, \quad J \propto \frac{\Delta - eV/2}{\sin^2\sqrt{\frac{\Delta - eV/2}{eV_L}}}; \\
&\text{(III)} \quad eV > E_F, \quad J \propto \frac{V^{\frac{2}{3}}}{[\mathrm{Ai}(\eta^-)\mathrm{Bi}(\eta^+) - \mathrm{Ai}(\eta^+)\mathrm{Bi}(\eta^-)]^2}; \\
&\text{(IV)} \quad eV \gg eV_L, \quad J \propto V^{\frac{5}{6}} \exp\left[-\frac{4}{3}\left(\frac{V}{V_L}\right)^{\frac{1}{2}}\right].
\end{aligned} \tag{7}$$

For $eV > E_F$ the current is a monotonously decreasing function of the voltage.

If the carrier density is not small, Eq. (5) does not hold, and Eqs. (2)–(4) must be solved numerically. The resultant characteristic $J(V)$ is shown in Fig. 4 for different

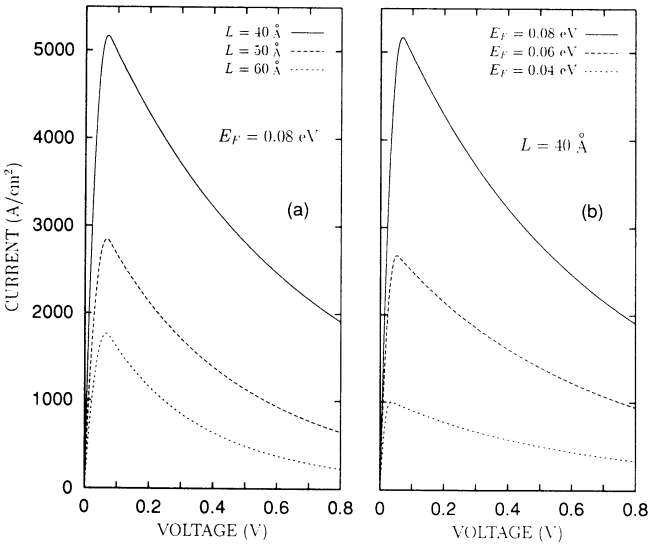

FIG. 4. The calculated zero-temperature current through an ITD as function of the bias voltage for different well widths L (a) and Fermi levels E_F (b). $\gamma = 1$. $E_F = 0.08$ eV corresponds to the highest carrier density reported to date (Ref. 5).

values of L and E_F, zero temperature, and fully penetratable interfaces ($\gamma = 1$). E_F as high as 0.08 eV, which correspond to hole densities of 2×10^{19} cm^{-3}, have already been achieved[5] by doping of Ge in the GaSb electrodes.

The results exhibit all the physical considerations discussed above. The four regimes depicted in Eqs. (7) are apparent also for high carrier densities. The peak current is of the order of 5×10^3 A cm^{-2}, which is of practical value. It is not far from the peak current observed in resonant ITD's.[4] The reason for this is the relative narrowness of the well. The zero current observed in the only experiment reported for narrow-well structures[6] can be understood from Fig. 4(b), as the carrier density in the experiment was two orders of magnitude smaller than in the present calculation.

In summary, we investigated the tunneling process in interband tunneling devices, in view of the peculiar boundary conditions of extreme type-II heterojunctions. We used a realistic effective-mass-approximation approach. The current through a narrow structure is found to behave nonlinearly with the voltage, exhibiting Ohm's-law behavior at small voltage and large negative differential resistance at higher voltages. This nonresonant NDR is basic to the structure, and is robust to changes such as imperfections and finite temperatures. It should be experimentally observed in all symmetric ITD's, including polytype structures with AlSb barriers separating the active materials.

[1] J. R. Söderström, D. H. Chow, and T. C. McGill, Appl. Phys. Lett. **55**, 1094 (1989).
[2] L. F. Luo, R. Beresford, and W. I. Wang, Appl. Phys. Lett. **55**, 2023 (1989).
[3] K. Taira, I. Hase, and H. Kawai, Electron. Lett. **25**, 1708 (1989).
[4] K. F. Longenbach, L. F. Luo, and W. I. Wang, Appl. Phys. Lett. **57**, 1554 (1990).
[5] K. F. Longenbach, L. F. Luo, S. Xin, and W. I. Wang, J. Cryst. Growth **111**, 651 (1991).
[6] E. T. Yu, D. A. Collins, D. Z.-Y. Ting, D. H. Chow, and T. C. McGill, Appl. Phys. Lett. **57**, 2675 (1990); D. Z.-Y. Ting, E. T. Yu, D. A. Collins, D. H. Chow, and T. C. McGill, J. Vac. Sci. Technol. B **8**, 810 (1990);
[7] D. Z.-Y. Ting, E. T. Yu, and T. C. McGill, Phys. Rev. B **45**, 3583 (1992).
[8] E. E. Mendez, J. Nocera, and W. I. Wang, Phys. Rev. B **45**, 3910 (1992).
[9] M. S. Kiledjian, J. N. Schulman, K. L. Wang, and K. V. Rousseau, Phys. Rev. B **46**, 16 012 (1992).
[10] M. A. Davidovich, E. V. Anda, C. Tejedor, and G. Platero, Phys. Rev. B **47**, 4475 (1993).
[11] A. Nogarat, M. A. Maldonado, R. E. Carnahan, K. P. Martin, F. Aristone, D. K. Maude, J. C. Portal, J. F. Chen, and A. Y. Cho, Phys. Rev. B **47**, 13 872 (1993).
[12] T. Ando and S. Mori, Surf. Sci. **113**, 124 (1982).
[13] W. A. Harrison and A. Kozlov (unpublished).
[14] C. B. Duke, in *Tunneling in Solids* in *Solid State Physics, Advances in Research and Applications*, edited by F. Seitz, D. Turnbull, and H. Ehrenreich (Academic, New York, 1969).

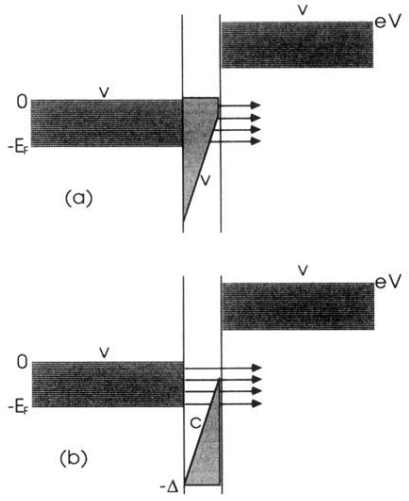

FIG. 2. Tunneling of holes in double heterojunction devices. (a) True tunneling (as in the GaAs-GaAlAs-GaAs system). (b) Interband tunneling. Shaded regions represent the true barriers, under which the quantum states are evanescent.

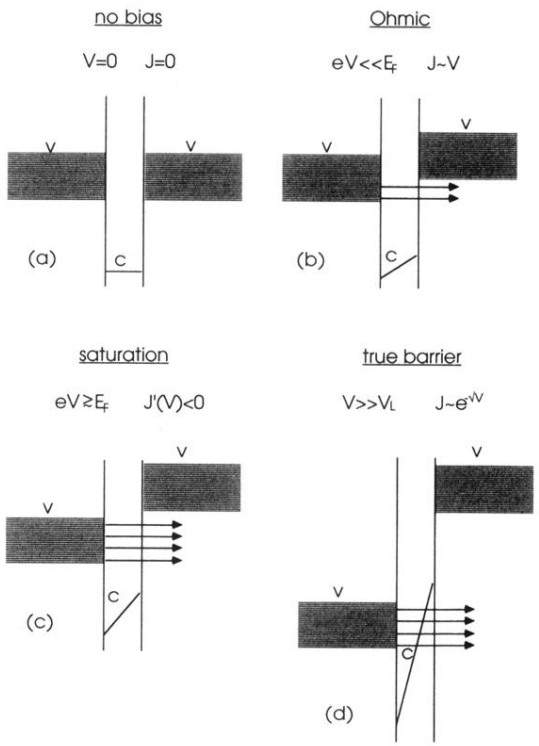

FIG. 3. The evolution of the energy profile of ITD with increasing voltage. Each snapshot represents a different regime in the J-V characteristics, as described in the text.